Ab initio study of phonon-induced dephasing of plasmon excitations in silver quantum dots

Zhenyu Guo,[1,2] Bradley F. Habenicht,[2,3] Wan-Zhen Liang,[1] and Oleg V. Prezhdo[2,*]
[1]*Department of Chemical Physics, University of Science and Technology of China, Hefei 230020, China*
[2]*Department of Chemistry, University of Washington, Seattle, Washington 98195, USA*
[3]*Department of Chemical and Biomolecular Engineering, University of Tennessee, Knoxville, Tennessee 37996, USA*
(Received 20 August 2009; revised manuscript received 14 January 2010; published 16 March 2010)

Phonon-induced pure dephasing of electronic excitations in silver quantum dots (QDs) is investigated with *ab initio* molecular dynamics at ambient and low temperatures. Three types of electronic states are studied corresponding to bulk, surface, and plasmon excitations. The electron-phonon coupling is strongest for bulk states and decreases for surface and plasmon states. The plasmon states dephase within 30–40 fs, which is consistent with the recent experiments [M. Z. Liu, M. Pelton, and P. Guyot-Sionnest, Phys. Rev. B **79**, 035418 (2009)]. The dephasing time shows weak dependence on the QD size but changes significantly with temperature. The bulk, surface, and plasmon states couple primarily to low-frequency acoustic phonons.

DOI: 10.1103/PhysRevB.81.125415 PACS number(s): 78.67.Bf

I. INTRODUCTION

Noble-metal nanoparticals have attracted intense interest in many area of modern science and technology, including nanophotonics, molecular electronics, biological imaging, surface-enhanced Raman scattering (SERS), photovoltaics, etc.[1–10] In contrast to bulk materials, plasmon states in metal nanoparticles can be tuned in energy by variations in particle size and shape, leading to plasmon resonances that can be excited by light of a well-defined wavelength. The energy and width of the plasmon resonances play key roles in the above applications. The resonance width gives the range of the light wavelengths that can be used technologically. It also limits the energy and number of molecular states whose optical activity is enhanced by interactions with the metal surface. The linewidths are determined by plasmon dephasing times, which have gained significant interest both experimentally and theoretically.[11–13] The homogeneous dephasing time is an important parameter in many applications. For instance, the effectiveness of optical switches, SERS, and optical tweezers[3,5,14,15] depend on the plasmon dephasing time. Therefore, one needs to clarify all mechanisms that are responsible for the ultrafast plasmon dephasing in metal quantum dots, including electron-surface scattering, electron emission, and electron-phonon interaction.

It is generally established that the fastest contribution to plasmon dephasing in metal nanoparticles is due to the purely electronic interaction between the plasmon state and the surface electrons.[11,16,17] In contrast, the optical linewidths of semiconductor nanocrystals are dominated by the electron-phonon interactions.[18,19] One may expect that electron-phonon interactions should also play an important role in the dephasing of the plasmon excitations. Only a few groups have studied the phonon-induced plasmon dephasing in metal nanoparticals. Compared to the dephasing resulting from electron-electron interactions, the phonon-induced dephasing should show a strong temperature dependence since the energies of the phonon modes of the metal nanoparticles are lower than the thermal energy at room temperature. As early as 1974, Kreibig[20] investigated the temperature dependence of the plasmon linewidths for silver clusters. However, strong *d*- and *sp*-band electronic transitions dominated the observed linewidths for the 3 eV resonance in the spherical silver particles. More recently, El-Sayed and co-workers[21] studied the temperature effects on the plasmon absorption for gold nanopaticles in water. Small temperature dependence have been observed over a moderate temperature interval from 18 to 72 °C. Last year, Guyot-Sionnest and co-workers[22] investigated the temperature variation in the dephasing rates of surface plasmons in gold nanoparticles over a broad temperature range. They found reduced dephasing rates at low temperatures, indicating that phonon motions generate a significant contribution to the overall plasmon dephasing process.

Semiphenomenological models describing the electron-electron[16,17] and electron-phonon[23,24] scattering contributions to plasmon damping in bulk metals have been developed as early as 1950s. Recent *ab initio* calculations show how plasmonic bands in larger metal clusters arise from single-particle excitations detectable in small clusters due to electron-electron interactions.[25–27] The collective electronic properties appear already in clusters containing several dozen atoms. Surprisingly, no *ab initio* atomistic studies of phonon-induced dephasing in metallic nanoparticles have been reported thus far. Phenomenological models and atomistic calculations complement each other. The former can describe a broad range of measurements and provide valuable physical insights. At the same time, phenomenological models make multiple assumptions and obtain parameters by fitting the experimental data. *Ab initio* calculations make few assumptions and do not contain parameters that are fitted directly to the experimental data. A moderate amount of fitting is made at the fundamental level of individual atoms. Atomistic studies are able to provide fine details of the considered processes and, in particular, to identify specific phonon modes that couple to the electronic excitations and to characterize explicitly the electron-phonon coupling for different excitation types.

In this paper, we present an *ab initio* study of the electron-phonon contribution of the homogeneous rate of pure dephasing of plasmon excitations in silver nanoclusters. The results illustrate that the phonon-induced dephasing mechanism is responsible for a notable contribution to the overall

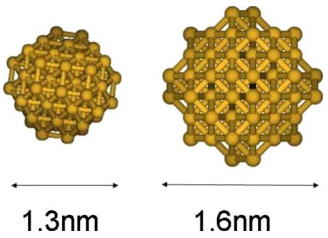

FIG. 1. (Color online) Geometry of Ag_{68} and Ag_{104} clusters with diameters as marked.

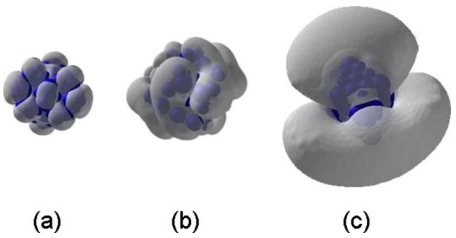

FIG. 2. (Color online) Electron density of the lowest-energy (a) bulk, (b) surface, and (c) plasmon states in the Ag_{104} cluster.

plasmon dephasing rate and linewidth. At the same time, the elastic electron-scattering mechanism of dephasing remains the dominant effect. The phonon contribution is about four to five times smaller than the electronic contribution. In addition to plasmons, we investigate the lower-energy electronic excitations localized inside the nanoclusters as well as on their surface. Dephasing of the bulk and surface states proceeds several times faster than the plasmon states. All three types of states are coupled primarily to low-frequency acoustic phonons that are particularly sensitive to the temperature variation.

II. THEORY

The simulations were performed with two silver clusters, Ag_{68} and Ag_{104}, with diameters of 1.3 and 1.6 nm, respectively, Fig. 1. The pure-dephasing times were calculated at low and room temperatures with *ab initio* molecular dynamics (MD). A standard technique for creating approximately spherical clusters and studying their properties was used. The original geometries of the clusters were obtained from the bulk structure of silver using a spherical cutoff. All atoms in a bulk crystal within this cutoff distance from a selected atom were included in the cluster. Then the cluster geometries were optimized at 0 K. Such geometry optimization created a significant relaxation of the atoms due to finite size and surface effect. The electronic structure of the optimized clusters was computed using *ab initio* density-functional theory, as implemented with the Vienna *ab initio* simulations package (VASP).[28,29] The Perdew-Burke-Ernzerhof functional[30] was used in order to describe the electron exchange and correlation interactions. All valence-shell electrons were treated explicitly while the core electrons were modeled with the projector-augmented-wave pseudopotentials.[31] A converged plane-wave basis was used in all calculations. Following the study of the optimized clusters, we generated MD trajectories at 50 and 300 K. The clusters were heated to the desired temperature by repeated velocity rescaling. Then microcanonical MD trajectories were generated using the Verlet algorithm with a 1 fs time step, as implemented within VASP.[28]

The line-shape theory for optical absorption and emission has been well developed.[32] The observed optical linewidths can be separated into several contributions. Inhomogeneous broadening arises from different local environments in a chromophore ensemble. At the single-particle level, neglecting the inhomogeneous broadening, the linewidths are determined by the sum of the population relaxation and pure-dephasing rates. The sum gives the homogeneous contribution to the linewidth,

$$\Gamma = \frac{1}{T_2} = \frac{1}{2T_1} + \frac{1}{T_2^*}. \quad (1)$$

Here, T_1 is the population relaxation time and T_2^* is the pure-dephasing time. If pure dephasing is much faster than population relaxation, as is the case with many types of chromophores, the homogeneous linewidth is determined by the pure-dephasing time. Recent experiments[33–38] have shown that the electron-phonon relaxation of plasmon excitations in metallic nanoclusters occurs on the time scale of about 1 ps, which is significantly longer than the pure-dephasing time. Therefore, the phonon contribution to the plasmon linewidths is determined by the inverse of the pure-dephasing time.

III. RESULTS AND DISCUSSION

A. Bulk, surface, and plasmon states

Figure 2 illustrates the three types of electronic states in the Ag_{104} cluster. It shows the spatial densities of the lowest-energy states of each type. The states clearly differ in their localization with respect to the silver atoms. In order to emphasize this difference further, Fig. 3 presents the projection of the three types of states along an arbitrary axis passing through the particle center. The localizations of the electronic states allow us to classify them as bulk, surface, and plasmon states. This nomenclature is rather approximate for the small clusters considered here and it is adopted for convenience of further discussion. The highly delocalized orbitals labeled here as plasmon states are often called "nearly-free-electronlike" and "superatom" states.[39]

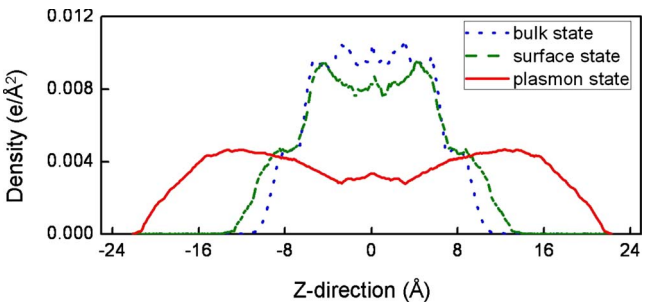

FIG. 3. (Color online) Cross sections of the electron densities shown in Fig. 2.

Similarly to the bulk material, the bulk states of the nanocluster are almost entirely localized on the silver atoms, Fig. 2. The range of the electron density for the bulk states, Fig. 3, is almost identical to the size of the cluster, Fig. 1. The surface states differ from the bulk states by an additional contribution from the unsaturated chemical bonds of the surface silver atoms. The density of the core region of the surface state is depleted compared to that of the bulk state, Fig. 3. Although the projected densities of the bulk and surface states appear to be quite similar in Fig. 3, these states indeed form distinct types, which becomes more clear in the three-dimensional Fig. 2. The plasmon states are unlike both bulk and surface states. Their densities extend far beyond the nanoparticle. Even in the relatively small clusters considered in this work, the majority of the plasmon state density is located predominantly in vacuum, and the density of the core region is greatly depleted.

The lowest-energy excitations in the silver nanoparticles are bulk states, see Table I. Surface states are 1.5 eV above the Fermi energy or higher. Plasmon states start at about 4 eV in the small silver clusters investigated here. Bulklike states can be found within the energy range of the surface states. All three types of states are present at the highest energies.

B. Active phonon modes

Fourier transforms (FTs) of the time-dependent energy of the electronic states along the MD trajectory characterize the phonon motions that cause the electronic dephasing.[18,40,41] The FTs show a significant spectral density only for those phonon modes that are strongly coupled to the electronic states. The resulting spectral density plots are presented in Fig. 4. The FT resolution is 33 cm^{-1}, as limited by the length of the MD trajectories. The plots show that only the low-frequency acoustic modes influence the electronic energies. The result is similar to the calculations performed with the semiconducting nanoclusters[18,19] and can be rationalized by the fact that the slow acoustic modes modulate the size and shape of the cluster. Such large-scale motions couple strongly to the electronic states since the state densities extend over the whole cluster. Changing cluster size or shape affects the electronic-state wave functions and changes the state energies. Indeed, the control of the nanocluster electronic spectra is achieved precisely by changes in the cluster size and shape. In contrast, the high-frequency optical modes involving local displacements of atoms with respect to each other have little effect on the global nanocluster properties, including the energies of the delocalized electronic states.

The low-frequency phonon modes couple to all three types of states: bulk, surface, and plasmon, Fig. 4. The strength of the electron-phonon coupling is different for the three states. The amplitude of the spectral density is notably smaller for the plasmon states, indicating that they couple to phonons much more weakly than the bulk and surface states. The electron-phonon interaction is weak because the plasmon states are localized away from the cluster, see Figs. 2 and 3. The states are largely detached from the silver atoms, and therefore, the atomic motions have small effect on the state properties.

TABLE I. Phonon-induced dephasing times of electronic states in silver QDs, computed by the direct, τ_d, and cumulant, τ_c, approaches, Eqs. (2) and (5), respectively. E is the state energy computed for the QD geometry optimized at zero temperature. $\langle E\rangle_T$ is the canonically averaged energy. The energies are given relative to the Fermi energy.

	τ_d (fs)	τ_c (fs)	E (eV)	$\langle E\rangle_T$ (eV)
Ag_{104} 300 K bulk	8.7	6.5	0.037	0.120
	8.3	6.6	0.257	0.305
	7.0	6.2	0.257	0.316
	13.2	13.5	0.429	0.423
	9.3	10.2	0.429	0.446
	9.3	10.2	0.429	0.447
Ag_{104} 300 K surface	15.6	14.6	1.465	1.446
	15.6	14.6	1.465	1.447
	14.1	14.3	1.465	1.450
	13.5	14.3	1.607	1.613
	15.9	17.8	1.607	1.620
Ag_{104} 300 K plasmon	27.6	26.5	3.952	3.955
	27.8	26.5	3.952	3.956
	27.5	26.5	3.952	3.956
	26.3	26.2	4.033	4.033
	36.2	35.5	4.033	4.042
	42.1	46.7	4.033	4.051
Ag_{104} 50 K plasmon	82.4	81.9	3.952	3.956
	74.2	75.8	3.952	3.955
	76.0	77.4	3.952	3.955
	29.4	32.3	4.033	4.019
	38.0	39.5	4.033	4.021
	58.6	61.0	4.033	4.035
Ag_{68} 300 K plasmon	36.8	26.5	3.957	4.148
	36.6	25.9	3.957	4.154
	34.5	31.1	3.957	4.157
	47.7	31.5	3.970	4.184
	15.6	16.0	3.970	4.210
	15.3	16.2	3.970	4.216

C. Pure-dephasing functions

The phonon-induced pure-dephasing times for the bulk, surface, and plasmon states are computed by two different approaches.[32] In the direct method, the dephasing function is defined as

$$D(t) = \exp(i\omega t)\left\langle \exp\left[-\frac{i}{\hbar}\int_0^t E(\tau)d\tau\right]\right\rangle_T. \qquad (2)$$

$E(\tau)$ in the above formula is the instantaneous value of the excitation energy and $\omega=\langle E\rangle_T/\hbar$ is the thermally averaged excitation frequency. The direct dephasing function is complex, in general. However, its imaginary part is much smaller than the real part. In special cases, for instance, when the excitation energy E is constant, the dephasing function is

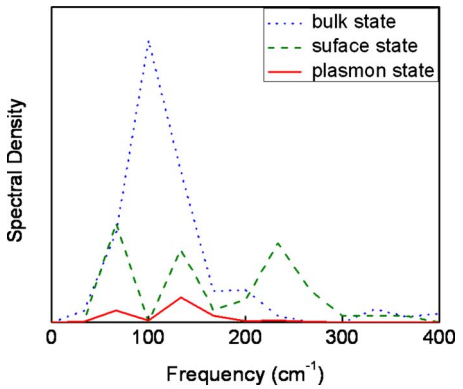

FIG. 4. (Color online) Fourier transforms of the energies of the electronic states shown in Fig. 2. The energies fluctuate due to phonon motions.

purely real, due to the presence of the phase prefactor $\exp(i\omega t)$. Below, we consider the real part of Eq. (2).

Additionally, the dephasing function can be calculated using the cumulant expansion.[32] The first-order cumulant vanishes. The second-order cumulant involves the autocorrelation function (ACF) of the fluctuation of the electronic-state energy relative to its thermally averaged value,

$$C(t) = \langle E(0)E(t)\rangle_T. \tag{3}$$

The cumulant dephasing function is obtained by doubly integrating the ACF,

$$g(t) = \int_0^t d\tau_1 \int_0^{\tau_1} d\tau_2 C(\tau_2) \tag{4}$$

and exponentiating the result,

$$D(t) = \exp[-g(t)]. \tag{5}$$

The dephasing functions computed using the above two methods for the lowest-energy bulk, surface, and plasmon excitations are shown in Fig. 5. The direct calculation converges more slowly than the cumulant approximation. However, it includes higher-order time correlations of the electron-phonon interaction while the cumulant approximation stops at the second-order ACF, Eq. (3). The direct and cumulant dephasing functions agree well within the first 10 fs, Fig. 5. The higher-order correlations become important at a later time. The cumulant approximation works best for the plasmon states, whose dephasing functions show little structure. The deviations are largest for the bulk states, for which a rapid oscillation in the direct dephasing function is superimposed on top of the overall decay. Generally, the cumulant functions decay more smoothly than the direct functions. The cumulant approximation works well because the phonons of the metallic clusters are quite harmonic and the anharmonic electron-phonon coupling is weak. The cumulant expansion works better with the plasmon states than surface and bulk states because the coupling is weaker for the plasmon states.

D. Pure-dephasing times

The pure-dephasing times τ are determined by fitting the dephasing functions [Eqs. (2) and (5)] by a Gaussian,

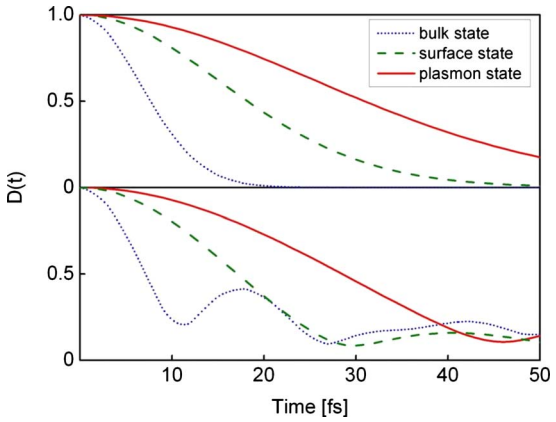

FIG. 5. (Color online) Pure-dephasing functions for the bulk, surface, and plasmon states shown in Fig. 2. The top panel shows the cumulant approximation result, Eq. (5) while the bottom panel depicts the direct result, Eq. (2). The dephasing times obtained by fitting the direct dephasing function to a Gaussian, Eq. (6), are presented in Table I for several lowest-energy bulk, surface, and plasmon states.

$$f(t) = \exp[-(t/\tau)^2/2]. \tag{6}$$

Table I presents the dephasing times for 5–6 lowest-energy bulk, surface, and plasmon states of Ag_{104} and Ag_{68} clusters at ambient and low temperatures. For the most part, the second-order cumulant approximation agrees with the direct calculation.

The pure-dephasing times for bulk, surface, and plasmon states are about 10, 15, and 30 fs, respectively, at room temperature. The differences in the dephasing times can be explained by the magnitudes of the electron-phonon coupling, reflected in the intensities of the spectral densities in Fig. 4. The bulk state has the highest spectral density, followed by the surface state. The spectral density of the plasmon state is the lowest. The electron-phonon coupling for the bulk state is stronger than that of surface and plasmon states. Therefore, the plasmon states show the longest dephasing times while the bulk states have the shortest dephasing.

Considering that the overall dephasing of plasmon excitations occurs within 10 fs, corresponding to a 65 meV homogeneous linewidth, our calculations show that the electron-phonon interaction contributes about 25–30 % to the plasmon linewidth. While the overall dephasing process is dominated by electron-electron scattering, the electron-phonon interaction constitutes a considerable effect. This theoretical result is consistent with the experimental data of Liu *et al.*[22]

E. Temperature, energy, and size dependences

Table I indicates that many of the electronic states are degenerate when Ag_{104} and Ag_{68} clusters are in their optimized geometry at 0 K, see the *E*, eV column of Table I. Thermal phonon motions lift the degeneracies, see the $\langle E\rangle_T$, eV column. As a result, the dephasing times of the states that are degenerate at 0° can differ notably at a finite temperature. One can see a significant variation in the phonon-induced

pure-dephasing times for different states of the same type. One can expect that the small size of the silver clusters enhances this variation, and makes the distinction between the bulk, surface, and plasmon states less pronounced compared to larger clusters.

In order to investigate the effect of the nanoparticle size and temperature on the plasmon dephasing, we studied both Ag_{68} and Ag_{104}, and performed MD calculations at 300 and 50 K. At the ambient temperature, the two clusters showed similar plasmon dephasing times, Table I. The deviations between direct and cumulant results were notably greater with the smaller cluster. The direct dephasing functions showed rather complicated structures, and the Gaussian fits, Eq. (6), were rather crude. The Gaussian fits of the cumulant functions were excellent for both the smaller and the larger silver particles. Comparing the cumulant results, one observes that the dephasing is somewhat faster in the smaller dot, which is consistent with the experiments.[11] Lowering the temperature had a significant effect on the dephasing time scale. The plasmon pure-dephasing times for Ag_{104} are about 30 and 80 fs at 300 and 50 K, respectively. These time scales translate to 21 and 9 meV phonon contributions to the plasmon linewidths.

IV. CONCLUSIONS

To recapitulate, using *ab initio* molecular dynamics, we have investigated the phonon contribution to the pure dephasing of plasmon excitations in small silver nanocrystals at ambient and low temperatures. The theoretical results are consistent with the experimental data obtained recently for gold nanoparticals at low and room temperatures. The simulations illustrate that the electron-phonon interaction for plasmon states is much weaker than that for nonplasmon states. This is because the plasmon states are localized away from the atoms, therefore, decreasing the Coulomb coupling between negative electrons and positive atomic cores. Additionally, the large size of the plasmon wave functions makes them less sensitive to the local atomic fluctuations, compared to the more localized nonplasmon wave functions. There exists a modest size dependence in plasmon dephasing, the plasmon damping for smaller dots is faster. This is manifestation of a general trend, by which electron-phonon interaction is stronger in small molecular systems and weaker in large bulk objects. Localized electronic excitations perturb atomic geometries to a larger extent. Both plasmon and nonplasmon states couple to low-frequency acoustic-phonon modes. High-frequency optical modes displace atoms relative to each other and carry little effect on the wave functions that are delocalized over the whole cluster. On the other hand, slow acoustic motions that change the shape and size of the clusters influence the properties of the electronic wave functions more significantly.

The simulations reported here were limited to small silver clusters in vacuum. We expect that the key conclusions summarized above should hold for other metals and for larger clusters interacting with an environment. One can anticipate that plasmon states, in particular, should be quite sensitive to environment since they extend far from the metal cluster. Phonon modes of a substrate or a medium hosting the clusters could also contribute to the dephasing of plasmonic excitations. The results indicate that the electron-phonon dephasing mechanism is an important part of the overall dephasing process, and that it creates a noteworthy contribution to the plasmon linewidth.

ACKNOWLEDGMENTS

The research was supported by grants from NSF under Grant No. CHE-0957280 and ACS-PRF under Grant No. 46772-AC6.

*Corresponding author; prezhdo@u.washington.edu

[1] R. C. Jin, Y. C. Cao, E. Hao, G. S. Métraux, G. C. Schatz, and C. A. Mirkin, Nature (London) **425**, 487 (2003).
[2] J. M. McLellan, Z.-Y. Li, A. R. Siekkinen, and Y. Xia, Nano Lett. **7**, 1013 (2007).
[3] P. K. Jain, X. Huang, I. H. El-Sayed, and M. A. El-Sayed, Acc. Chem. Res. **41**, 1578 (2008).
[4] A. L. Pyayt, B. Wiley, Y. Xia, A. Chen, and L. Dalton, Nat. Nanotechnol. **3**, 660 (2008).
[5] J. Zhao, A. O. Pinchuk, J. M. McMahon, S. Li, L. K. Ausman, A. L. Atkinson, and G. C. Schatz, Acc. Chem. Res. **41**, 1710 (2008).
[6] L. Au, D. Zheng, F. Zhou, Z.-Y. Li, X. Li, and Y. Xia, ACS Nano **2**, 1645 (2008).
[7] S. D. Standridge, G. C. Schatz, and J. T. Hupp, J. Am. Chem. Soc. **131**, 8407 (2009).
[8] J. Y. Lee, B. H. Hong, W. Y. Kim, S. K. Min, Y. Kim, M. V. Jouravlev, R. Bose, K. S. Kim, I.-C. Hwang, L. J. Kaufman, C. W. Wong, P. Kim, and K. S. Kim, Nature (London) **460**, 498 (2009).
[9] K. Ishizaki and S. Noda, Nature (London) **460**, 367 (2009).
[10] P. Zijlstra, J. W. M. Chon, and M. Gu, Nature (London) **459**, 410 (2009).
[11] J. Bosbach, C. Hendrich, F. Stietz, T. Vartanyan, and F. Trager, Phys. Rev. Lett. **89**, 257404 (2002).
[12] T. Zentgraf, A. Christ, J. Kuhl, and H. Giessen, Phys. Rev. Lett. **93**, 243901 (2004).
[13] I. D. Mayergoyz, Z. Zhang, and G. Miano, Phys. Rev. Lett. **98**, 147401 (2007).
[14] S. M. Nie and S. R. Emery, Science **275**, 1102 (1997).
[15] L. Novotny, R. X. Bian, and X. S. Xie, Phys. Rev. Lett. **79**, 645 (1997).
[16] R. N. Gurzhi, Sov. Phys. JETP **8**, 673 (1959).
[17] W. E. Lawrence and J. W. Wilkins, Phys. Rev. B **7**, 2317 (1973).
[18] H. Kamisaka, S. V. Kilina, K. Yamashita, and O. V. Prezhdo, Nano Lett. **6**, 2295 (2006).
[19] O. V. Prezhdo, Chem. Phys. Lett. **460**, 1 (2008).
[20] U. Kreibig, J. Phys. F: Met. Phys. **4**, 999 (1974).
[21] S. Link and M. A. El-Sayed, J. Phys. Chem. B **103**, 4212 (1999).
[22] M. Z. Liu, M. Pelton, and P. Guyot-Sionnest, Phys. Rev. B **79**,

035418 (2009).
[23] R. N. Gurzhi, Sov. Phys. JETP **6**, 506 (1958).
[24] T. Holstein, Ann. Phys. (N. Y.) **29**, 410 (1964).
[25] C. M. Aikens, S. Li, and G. C. Schatz, J. Phys. Chem. C **112**, 11272 (2008).
[26] D. J. Masiello and G. C. Schatz, Phys. Rev. A **78**, 042505 (2008).
[27] K. Baishya, J. C. Idrobo, S. Ogut, M. Yang, K. Jackson, and J. Jellinek, Phys. Rev. B **78**, 075439 (2008).
[28] G. Kresse and J. Furthmüller, Comput. Mater. Sci. **6**, 15 (1996).
[29] D. S. Kilin, O. V. Prezhdo, and Y. Xia, Chem. Phys. Lett. **458**, 113 (2008).
[30] J. P. Perdew, K. Burke, and M. Ernzerhof, Phys. Rev. Lett. **77**, 3865 (1996).
[31] P. E. Blochl, Phys. Rev. B **50**, 17953 (1994).
[32] S. Mukamel, *Principles of Nonlinear Optical Spectroscopy* (Oxford University Press, New York, 1995).
[33] O. L. Muskens, N. Del Fatti, and F. Vallee, Nano Lett. **6**, 552 (2006).
[34] G. V. Hartland, Annu. Rev. Phys. Chem. **57**, 403 (2006).
[35] J. H. Hodak, A. Henglein, and G. V. Hartland, J. Chem. Phys. **112**, 5942 (2000).
[36] W. Huang, W. Qian, M. A. El-Sayed, Y. Ding, and Z. L. Wang, J. Phys. Chem. C **111**, 10751 (2007).
[37] S. Park, M. Pelton, M. Liu, P. Guyot-Sionnest, and N. F. Scherer, J. Phys. Chem. C **111**, 116 (2007).
[38] J. Burgin, P. Langot, A. Arbouet, J. Margueritat, J. Gonzalo, C. N. Afonso, F. Vallée, A. Mlayah, M. D. Rossell, and G. Van Tendeloo, Nano Lett. **8**, 1296 (2008).
[39] J. Zhao, M. Feng, J. Yang, and H. Petek, ACS Nano **3**, 853 (2009).
[40] B. F. Habenicht, H. Kamisaka, K. Yamashita, and O. V. Prezhdo, Nano Lett. **7**, 3260 (2007).
[41] B. F. Habenicht, O. N. Kalugin, and O. V. Prezhdo, Nano Lett. **8**, 2510 (2008).